Chemical Engineering Journal 283 (2016) 999–1008

Contents lists available at ScienceDirect

Chemical Engineering Journal

journal homepage: www.elsevier.com/locate/cej

Augmenting the adsorption of palladium from spent catalyst using a thiazole ligand tethered on an amine functionalized polymeric resin

Shivani Sharma, N. Rajesh *

Department of Chemistry, Birla Institute of Technology and Science, Pilani-Hyderabad Campus, Jawahar Nagar, Shameerpet Mandal, R.R. District, Hyderabad 500 078, India

HIGHLIGHTS

- 2-Mercaptobenzothiazole anchored onto amine functionalized polymeric resin for palladium adsorption.
- Physico-chemical characterization using FT-IR, SEM, EDX and optical imaging.
- The maximum Langmuir adsorption capacity of Pd(II) was 50.00 mg g^{-1}.
- The process is exergonic and endothermic.
- The method was tested to recover palladium from a catalyst.

GRAPHICAL ABSTRACT

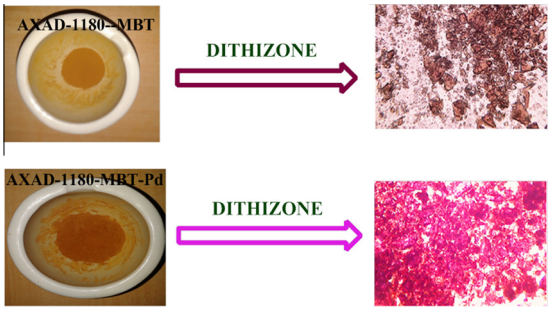

ARTICLE INFO

Article history:
Received 19 June 2015
Received in revised form 31 July 2015
Accepted 1 August 2015
Available online 28 August 2015

Keywords:
Palladium
Amberlite XAD resin
2-Mercaptobenzothiazole
Spent catalyst
Regeneration

ABSTRACT

Palladium is an industrially important precious metal and its recovery is of utmost significance in miscellaneous applications. Polystyrene divinylbenzene resins are known for their high surface area and porosity to effectively capture metal ions after suitable modification. In this work, we report the anchoring of 2-mercaptobenzothiazole onto the amine functionalized Amberlite XAD-1180 resin for the effective adsorption of palladium. The macroreticular resin serves as a good host to welcome palladium (guest) and the proof of concept was established comprehensively using FT-IR, SEM, EDX and optical imaging analysis. The Langmuir adsorption capacity of the functionalized resin for Pd^{2+} acquired through the linear isotherm model was found to be 50.00 mg g^{-1}. Kinetics of the adsorption process synchronized well with the pseudo-second order model and furthermore the exergonic and endothermic nature of the adsorption process was quantified through the negative free energy and positive enthalpy values. Regeneration of the resin surface was done using thiourea and the method was tested in recovering palladium from a spent catalyst containing 5% Pd on activated carbon.

1. Introduction

The Nobel Prize awarded to Suzuki, Heck and Negishi in 2010 has evoked considerable interest to understand and explore the prospective applications of palladium [1]. The favorable chemical and physical properties of platinum group metals have attracted widespread applications in jewellery, electronics, catalysis and pharmaceuticals [2]. The rapid industrial development resulting in the increasing demand for palladium has further enhanced the significance towards recovering this valuable metal [3–5]. Techniques such as solvent extraction, ion exchange, chemical precipitation and adsorption [6] are known for the recovery of palladium. Among these, solid phase extraction [7] is an effective strategy for the recovery of metal ions from aqueous solution and the selection of adsorbent plays a key role in it. Therefore, research on novel adsorbents has attracted considerable attention in analytical chemistry [8]. Modification of adsorbents through functionalization,

* Corresponding author. Tel.: +91 4066303503; fax: +91 4066303998.
E-mail address: nrajesh05@gmail.com (N. Rajesh).

http://dx.doi.org/10.1016/j.cej.2015.08.061
1385-8947/

grafting and impregnation techniques are quite appropriate for the adsorption of palladium [9].

Polymeric resins have attracted huge attention due to their macroreticular nature that enhances the adsorption capacity and chelating site accessibility for various metal ions [10,11]. Ligands with functional groups or suitable donor atoms containing sulfur and nitrogen have been developed for the adsorption of various metal ions including palladium.

Amberlite XAD series of resins endowed with a polystyrene divinyl benzene matrix have proven to be an efficient support for anchoring chelating ligands due to their porosity, high surface area and excellent chemical and physical stability [10]. The resin in the native form does not possess any vital functional group and hence requires suitable modification in order to create active sites that would augment the interaction with metal ions.

Mladenova et al. [12] have reviewed the utility of diverse adsorbent materials for the recovery of precious metal ions such as gold(III), platinum(IV) and palladium(II), respectively. Amberlyst-A 21 and Amberlyst-A 29 anion exchange resins are known to adsorb palladium as its chloro-complex from acidic medium [13]. Similarly, Amberlite XAD-7 modified with ligands such as dimethylglyoxal bis-(4-phenyl-3-thiosemicarbazone) and glyoxal dithiosemicarbazone [14] also show good potential to adsorb palladium.

Amberlite XAD-16 functionalized with 2-acetyl pyridine group has been studied for the solid phase extraction and recovery of palladium from high level waste solution [15]. Cross-linked chitosan resin chemically modified with L-lysine has been utilized to examine the adsorption of Pt(IV), Pd(II), Au(III) from aqueous solutions [16]. Precious metals such as Pd, Au and Pt have been recovered using p-amino benzoic acid modified waste newsprint paper [17]. The interaction between chitosan and an ionic liquid such as Aliquat-336 has also proven to be effective for the adsorption of palladium [18].

Ligands containing sulfur and nitrogen as donor atoms are known to chelate with metal ions such as palladium and platinum [12]. The adsorption of palladium using sulfur containing ligand-biopolymer combinations such as 2-mercaptobenzothiazole impregnated cellulose [19] and 2-mercaptobenzimidazole anchored chitosan [20] has also been investigated and these sorbents show adsorption capacities of 5.0 and 19.2 mg g^{-1} respectively. However, the interaction of functionalized macroreticular Amberlite XAD resins with the above ligands has not been reported as on date. Hence, in order to enhance the adsorption capacity we report an effective novel method for the adsorption of an industrially important and precious metal palladium by coupling of the amine functionalized Amberlite XAD-1180 resin with 2-mercaptobenzothiazole. The method was also tested to recover palladium from a catalyst. The resin was thoroughly characterized using different analytical techniques followed by the optimization of vital adsorption parameters.

2. Materials and methods

2.1. Reagents and instrumentation

Analytical grade reagents were used in all the experiments. Milli Q water was used in the preparation of the working aqueous solutions of Pd(II) of different concentrations. Amberlite XAD-1180 resin (surface area of 450 m^2/g and pore volume 1.4 mL/g) and 2-mercaptobenzothiazole (MBT) were obtained from Sigma Aldrich and used as such without further purification. Nitric acid, sulfuric acid and hydrochloric acid were procured from Himedia, India. Stannous chloride ($SnCl_2$) and sodium hydroxide (NaOH) were obtained from S.d. fine Chemicals Limited, India. Sodium nitrite and palladium(II) chloride were procured from Merck, India. A working concentration of 40 mg L^{-1} Pd(II) was prepared by appropriate dilution from 1000 mg L^{-1} stock palladium solution.

The pH adjustments of the aqueous solutions were done after calibration with pH 4.0 and 7.0 buffer solutions using an Elico Li-127 model pH meter procured from Elico, India. Batch studies in conical flasks kept in an incubator shaker (Biotechnics, India) were equilibrated for the required time period. A Jasco 4200 FT-IR spectrometer was used to account for the various functional groups in resin functionalized mercaptobenzothiazole in the range 400–4000 cm^{-1}. The optical images of the resin surface were captured using an Olympus CH20i optical microscope using diphenylthiocarbazone as a color reagent for palladium. A Hitachi S-3400 model instrument was used to observe the morphological changes in the resin adsorbent through SEM and energy dispersive X-ray spectrum (EDX) from batch studies after the adsorption of palladium. The concentration of palladium in the aqueous phase was quantified using flame Atomic absorption spectrophotometry (Shimadzu, AA 7000; air-acetylene flame at wavelength 247.6 nm).

2.2. Functionalization of Amberlite XAD-1180 resin and synthesis of MBT-AXAD-1180

Amberlite XAD-1180 resin was functionalized using the method reported earlier [11,21]. A 5.0 g weight of Amberlite XAD-1180 resin was taken in a round bottom flask and concentrated nitric (10 mL) and sulfuric (25 mL) acid were added and the reaction mixture was kept for stirring at 60 °C for 1 h on a water bath. Next, the reaction mixture was poured into an ice–water mixture. The nitrated resin was filtered, washed with water until it was acid free and further added to a reducing mixture of 40 g of $SnCl_2$, 45 mL of concentrated HCl and 50 mL of ethanol. The system was refluxed for 12 h at 90 °C on an oil bath. The solid precipitate was filtered, washed with water and 2.0 mol L^{-1} NaOH. The aminated resin was firstly washed with 2.0 mol L^{-1} HCl and finally with distilled water to remove excess of HCl. For diazotization, the amino resin was suspended in 50 mL of a 6.0 mol L^{-1} HCl solution at 0–5 °C. A solution of 2.1 g of sodium nitrite in 20 mL of water was added drop wise. The mixture was stirred and kept at 0–5 °C for 1 h. The diazotized resin was filtered off and washed with ice-cold water.

For coupling, 4.0 g of 2-mercaptobenzothiazole was added to 40 mL of 1.0 mol L^{-1} NaOH solution and the mixture was cooled to 0–5 °C. This solution was added drop wise to the above diazotized resin with vigorous stirring. The resulting mixture was refrigerated at 0–5 °C. The dark-brown resin was filtered, washed with water and dried in air.

2.3. Batch adsorption experiments

The batch studies were performed by equilibrating 0.1 g of the amine functionalized resin-MBT adsorbent containing 30 mL of 40 mg L^{-1} palladium(II) solution at pH 4.0 in a conical flask at room temperature (25 °C) for the desired time interval in an orbital incubator shaker (Biotechnics, India) at 110 rpm. The concentration of palladium in the aqueous phase was analyzed using flame atomic absorption spectrophotometry (Shimadzu Model AA 7000) at 247.6 nm with an acetylene-air flame as the fuel-oxidant combination. The amount of palladium(II) adsorbed at equilibrium (q_e) is calculated using the relation

$$q_e = (C_0 - C_e) \times \frac{V}{W} \quad (1)$$

where V is the volume of the solution (L), W is the weight of the resin adsorbent used (g), and C_0 and C_e are the initial and equilibrium liquid phase concentrations of palladium respectively. Experiments

were performed in triplicate and the adsorption process was studied using first order and second-order kinetics and the isotherm was evaluated using the Langmuir and Freundlich models.

3. Results and discussion

3.1. FT-IR characterization

The FT-IR spectra (Fig. 1) showed characteristic bands corresponding to the various functional groups in nitrated, aminated, Amberlite XAD-1180-MBT and Pd(II) treated resin adsorbent. The study showed characteristic bands at 3420 and 3438 cm^{-1} (aromatic C–H stretching), 2892 and 2922 cm^{-1} (aliphatic C–H stretching) [22]. In the spectrum of nitrated resin, the bands at 1573 and 1301 cm^{-1} are ascribed to asymmetric (N–O) and symmetric (N–O) stretching [23]. After the reduction of nitrated resin, the peak at 1573 cm^{-1} disappeared due to the formation of amine functional group [24]. A peak at 3400 cm^{-1} is attributed to the water adsorbed to the resin and 1617 cm^{-1} could be ascribed to the N–H vibrations in aminated resin. The nitro and amine groups have a nitrogen atom attached to a carbon (C–N). However, nitro group being more bulky than the amino group requires higher energy to resonate. This explains the shift in frequency from 1301 to 1359 cm^{-1} [24]. When diazotized resin was treated with 2-mercaptobenzothiazole (2-MBT), the peak at 1359 cm^{-1} disappeared as the functional group is bulky. Peaks at 1625 and 1425 cm^{-1} arise due to modification of resin by the ligand and are characteristic of N–H [25] and N=N vibrations respectively. Peak at 752 cm^{-1} could be ascribed to C–S stretching in MBT. The IR spectrum of the free chelating resin was compared with the spectrum of palladium ion saturated resin. A shift is observed in the N–H band from 1625 to 1694 cm^{-1} which suggests that chelation through N–H group is probably responsible for palladium sorption. Appearance of a peak due to C–S stretching is also evident at 705 cm^{-1} [25]. All these features illustrate that Pd(II) exhibits good interaction with the S and N atoms of MBT anchored onto the amine functionalized resin surface.

3.2. Morphological changes (optical images and scanning electron microscopy) and energy dispersive X-ray analysis

The scanning electron microscopy (SEM) images show certain morphological changes in the functionalized resin adsorbent and Pd(II) treated adsorbent (Fig. 2). The SEM images were obtained by applying an accelerating voltage of 20,000 V with 500× and 1000× magnification. In the SEM image of resin adsorbent, a solid and consistent surface pattern is observed and after adsorption of palladium, smaller agglomerated particles are visible in a porous matrix indicating the plausible interaction between 2-mercaptobenzothiazole anchored onto amine functionalized resin and Pd(II). This could be ascribed to the adsorption of Pd(II) onto the surface of resin adsorbent. To further validate the adsorption of palladium onto the porous resin matrix, optical images and energy dispersive X-ray analysis were also recorded. The optical microscopy images of the AXAD-1180-MBT adsorbent (Fig. 2A) and adsorbent treated with Pd(II) (Fig. 2B) were recorded by spreading the resin adsorbent and Pd(II) treated adsorbent on a glass slide using 4× magnification. The difference in the image was visualized by adding dithizone (a chelator for palladium) before and after adsorption. The change in the surface morphology (Fig. 2B) to a distinct pink-violet color (due to Pd-chelate) signifies that palladium is adsorbed effectively on the resin surface [19].

Supplementary evidence was ascertained through the EDX analysis of the resin surface before and after palladium adsorption (Fig. 3). The EDX spectrum of the resin surface (Fig. 3) indicates the presence of carbon, oxygen, sulfur and chlorine. After adsorption onto the MBT functionalized resin surface, the presence of palladium could be observed in the range of 2.5–3.0 keV [18–20] along with the other peaks (Fig. 3).

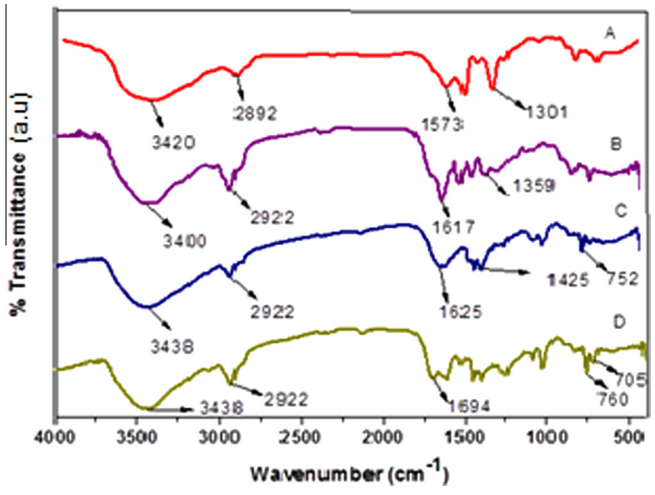

Fig. 1. FT-IR spectrum of nitrated (A), aminated (B), functionalized resin (C) and Pd (II) treated resin adsorbent (D).

3.3. pH effect and amount of adsorbent

The pH of aqueous phase was varied over the range 2–7 prior to equilibration. The optimum pH for the adsorption of palladium was observed at pH 4.0 (Fig. 4A) favoring the effective interaction of palladium through the sulfur and nitrogen donor atoms of MBT in the resin surface. At pH values less than 4.0, the competition from H^+ ions for the active adsorption sites would reduce the ligation interaction of S and N with the metal ion and hence the percentage adsorption is quite less. Above pH 4.0, the percentage adsorption of palladium showed a decrease and this could be assigned to the competition of hydroxyl species such as $PdCl_2(OH)^{2-}$, $Pd(OH)_2$, and $Pd(OH)_4^{2-}$ for the active adsorption sites [26]. The scheme illustrating the resin preparation and interaction with palladium is shown in Fig. 4B.

The amount of resin adsorbent used in the batch study was varied in the range 0.01–0.3 g (Fig. 4C). The percentage adsorption was found to be maximum (93.0 ± 0.2%) with three replicate measurements with the resin adsorbent in the range 0.1–0.3 g in 30 mL sample volume. Beyond 0.3 g, there was no appreciable increase in the percentage adsorption which could be attributed to the saturation of the active adsorption sites on the AXAD-1180-MBT surface.

3.4. Adsorption isotherm studies

3.4.1. Langmuir adsorption isotherm

Langmuir isotherm model adopts uniform adsorption and describes monolayer adsorption on a surface containing a limited number of identical sites [27,28]. This isotherm portrays the relation between the equilibrium concentration of the palladium C_e and the amount adsorbed at equilibrium (q_e) on the resin surface). The Langmuir isotherm model was used to acquire the maximum adsorption capacity, which is calculated as the amount of palladium(II) adsorbed per unit weight of the resin adsorbent. By fitting the experimental data (Table S1 of Supporting Information) to Langmuir isotherm model, various isotherm parameters were obtained from the linear and non-linear Langmuir equations expressed as

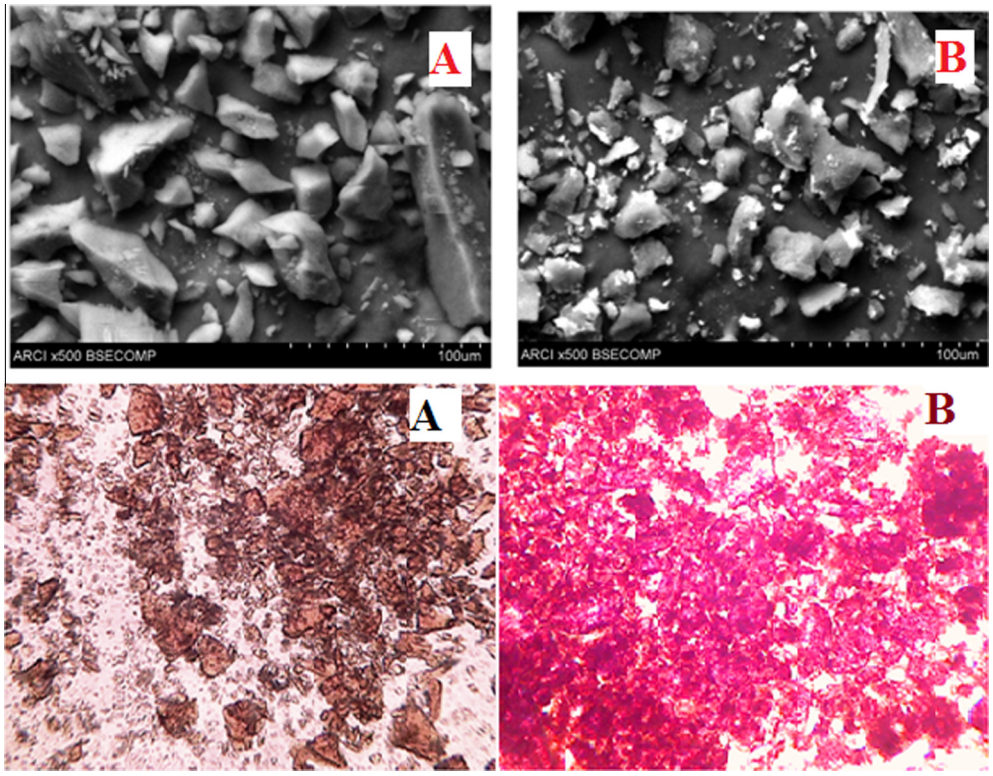

Fig. 2. SEM and optical images of (A) resin adsorbent and (B) Pd(II) treated resin adsorbent.

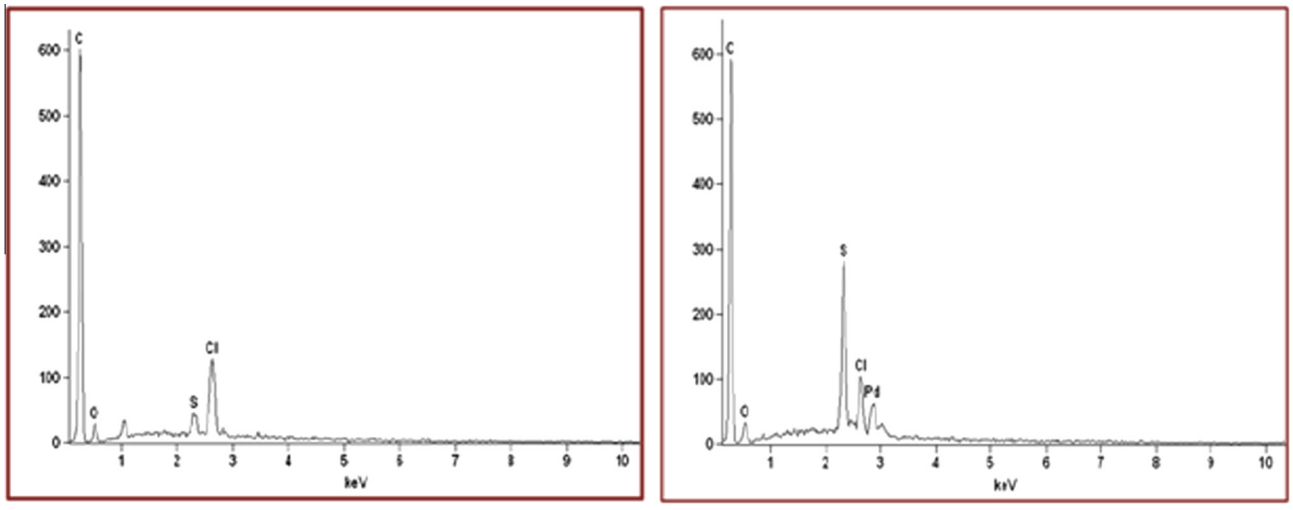

Fig. 3. EDX spectrum of the resin adsorbent and Pd(II) treated resin adsorbent.

$$\frac{C_e}{q_e} = \frac{1}{q_0 b} + \frac{C_e}{q_0} \quad (2)$$

$$q_e = \frac{q_0 b C_e}{1 + b C_e} \quad (3)$$

where C_e is the equilibrium concentration of palladium in mg L^{-1}, q_e is the amount of Pd(II) adsorbed at equilibrium in mg g^{-1}, q_0 is the maximum adsorption capacity in mg g^{-1}, and b is a constant (L mg^{-1}) related to the adsorption energy. The maximum adsorption capacity, q_0 and the constant b were obtained from the Langmuir linear and non-linear plots (Fig. 5A and C). The regression coefficient obtained from the linear and non-linear plot was found to be 0.99 and 0.93, respectively and the respective isotherm parameters are shown in Table 1. The implication of linear isotherm model is quite obvious from the higher adsorption capacity (50.0 mg g^{-1}) as well as the larger correlation coefficient. In order to forecast the suitability of an adsorption system, an important parameter called the dimensionless separation factor R_L was calculated [29] using the equation ($R_L = 1/1 + bC_0$), where C_0 is the initial concentration (40 mg L^{-1}) of palladium(II) and b is the Langmuir constant (L mg^{-1}). If R_L value is zero, then it accounts for irreversible adsorption while values greater than 1 indicate poor or unfavourable adsorption. The value of R_L for the adsorption of palladium on the Amberlite XAD-1180-MBT adsorbent was found to be less than 1 for linear and non-linear plots and this is an index

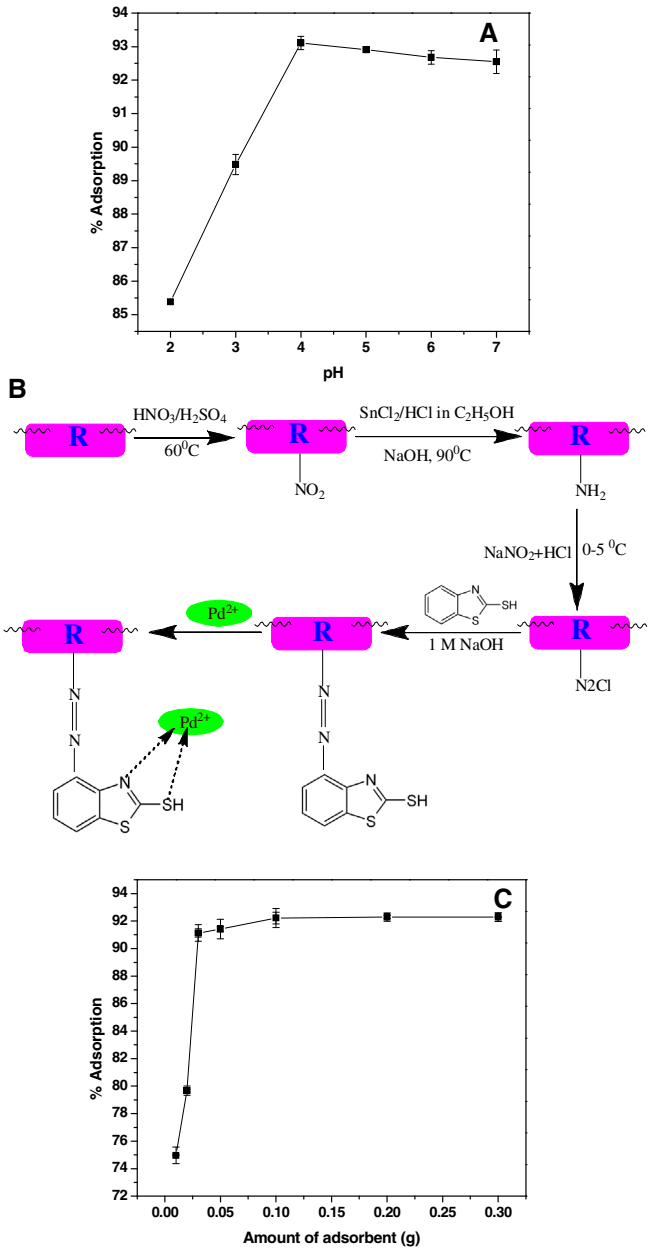

Fig. 4. Effect of (A) pH, (B) scheme illustrating the resin preparation and interaction with palladium and (C) dosage of adsorbent.

to the good fit to Langmuir isotherm as well as effectiveness of interaction between palladium(II) and the resin adsorbent surface under the given experimental conditions.

3.4.2. Freundlich isotherm

The Freundlich isotherm based on sorption on a heterogeneous surface [30] also serves as an alternative useful model to assess the adsorption from dilute solutions. The linear and non-linear expression correlating equilibrium adsorption capacity can be expressed as

$$\log q_e = \log K_F + \frac{1}{n} \log C_e \tag{4}$$

$$q_e = K_F C_e^{1/n} \tag{5}$$

where C_e is the equilibrium concentration of the Pd(II) ion in mg L^{-1}, q_e is the amount of palladium(II) adsorbed at equilibrium in mg g^{-1}, K_F and n are the Freundlich constants for adsorption capacity and the adsorption intensity respectively. The values of K_F and n were obtained from the Freundlich linear and non-linear plots (Fig. 5B and C). The linear isotherm model has a higher correlation coefficient (0.80) as compared to the non-linear fit. The C_e and q_e data for the plots is given in Table S1 of Supporting Information and the isotherm parameters are presented in Table 1. For a constructive or favorable adsorption process the Freundlich constant n would be in the range 1–10 and larger the value, more effective is the resin adsorbent-palladium interaction [31,32].

3.5. Kinetics of adsorption

The kinetics of the palladium adsorption onto the resin surface was studied using first-order [33] and pseudo-second order [34] models and the linearized equations are expressed as

$$\log (q_e - q_t) = \log q_e - \frac{k_1 t}{2.303} \tag{6}$$

$$\frac{t}{q_t} = \frac{1}{k_2 q_e^2} + \frac{t}{q_e} \tag{7}$$

where q_e and q_t refers to the amount of palladium adsorbed at equilibrium and time t with the first and second-order rate constants k_1 and k_2, respectively. By fitting the experimental data (Table S2 of Supporting Information) through the linear plots of log $(q_e - q_t)$ and t/q_t against t (Fig. 6A and B), respective kinetic parameters were obtained for the above models. The adsorption data synchronized well with the pseudo-second-order model because of the higher regression coefficient (Table 2). The q_e values obtained experimentally and from the second-order kinetic model were found to be 11.304 and 11.176 mg g^{-1} respectively. The proximity of the experimental and calculated q_e values testifies the applicability of second-order model in understanding the adsorption kinetics of palladium onto the functionalized resin surface. The overall rate of adsorption of palladium on the AXAD-1180-MBT adsorbent could be influenced by (a) film or surface diffusion, where Pd(II) is transported from the bulk solution to the external resin adsorbent surface (b) intraparticle or pore diffusion, where the adsorbate Pd molecules move into the interior of the resin adsorbent particles and (c) Pd(II) adsorption on the interior sites of the resin adsorbent [35,36]. Since, the adsorption step is fairly rapid, it is assumed that it does not bear profound influence on the adsorption kinetics. Therefore, the overall rate of palladium adsorption onto the functionalized resin could be controlled by either surface or intraparticle diffusion. The Weber-Morris [37] intraparticle diffusion model is appropriate to conclude whether intraparticle diffusion is the rate-determining step. According to the W–M model, a plot of q_t versus $t^{½}$ would be linear if intraparticle diffusion is implicated in the adsorption process and furthermore, if the plot cuts through the origin then intraparticle diffusion is the only rate-limiting step. The plot of q_t against the square root of time yields a finite intercept (Fig. 6C) and this indicates that boundary layer mechanism [38] could also be involved in following the adsorption kinetics of Pd(II) onto the AXAD-1180-MBT interface.

3.6. Thermodynamics of adsorption

The thermodynamics that influences the transport of Pd(II) onto the functionalized resin surface is governed by the concentration gradient across the resin adsorbent-solution interface. This results in the difference in the free energy between the resin surface and solution phase as

$$\Delta G^0 = -RT \ln \frac{[Pd]_{\text{resin surface}}}{[Pd]_{\text{solution phase}}} \tag{8}$$

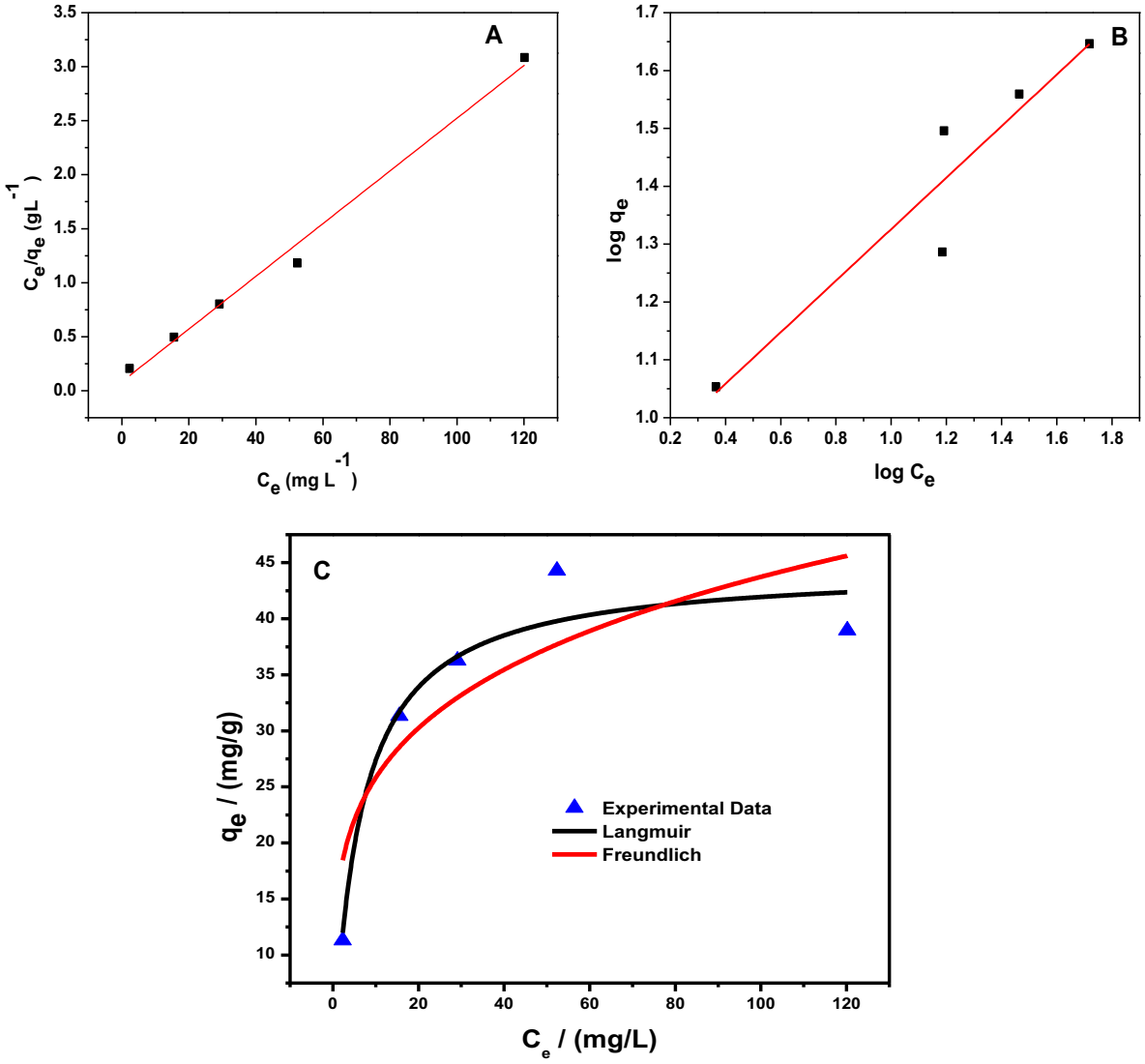

Fig. 5. (A) Langmuir isotherm, (B) Freundlich isotherm and (C) non-linear Langmuir and Freundlich isotherm plots.

Table 1
Equilibrium isotherm models.

Isotherm model		Parameters	Values
Langmuir	Linear	q_0 (mg g^{-1})	50.00
		b (L mg^{-1})	0.240
		R_L	0.094
		R^2	0.98
	Non-linear	q_0 (mg g^{-1})	44.58
		b (L mg^{-1})	0.158
		R_L	0.136
		R^2	0.93
Freundlich	Linear	K_F (mg$^{1-1/n}$ g^{-1} L$^{1/n}$)	10.125
		n	2.941
		R^2	0.80
	Non-linear	K_F (mg$^{1-1/n}$ g^{-1} L$^{1/n}$)	15.225
		n	4.3642
		R^2	0.67

The $[Pd]_{resin\ surface}$ is greater than $[Pd]_{solution\ phase}$ at equilibrium. The overall free energy would be negative. This results in the spontaneous adsorption and a higher K value. Furthermore in terms of chemical potential, μ

$$\mu_{Pd(II)} = \mu^{o}_{Pd(II)} + RT \ln a_{Pd(II)} \quad (9)$$

For dilute solutions, a α C, therefore

$$\mu_{Pd(II)} = \mu^{o}_{Pd(II)} + RT \ln C_{Pd(II)} \quad (10)$$

Now $[Pd]_{solution\ phase} \rightleftharpoons [Pd]_{resin\ surface}$

Hence,

$$\Delta G_{ads} = \Delta G^{o}_{ads} + RT \ln[Pd_{resin\ surface} - Pd_{solution\ phase}] \quad (11)$$

At equilibrium,

$$\Delta G_{ads} = 0,\ \Delta G^{0}_{ads} = -RT \ln \frac{[Pd]_{resin\ surface}}{[Pd]_{solution\ phase}} \quad (12)$$

Therefore,

$$\Delta G^{0}_{ads} = -RT\ \ln K$$

In order to comprehend the spontaneity and energetics of the adsorption process, the adsorption studies were carried out at varying temperatures (Table S3 of Supporting Information) and thermodynamic parameters including free energy, enthalpy and entropy changes were obtained from the following equations [39]

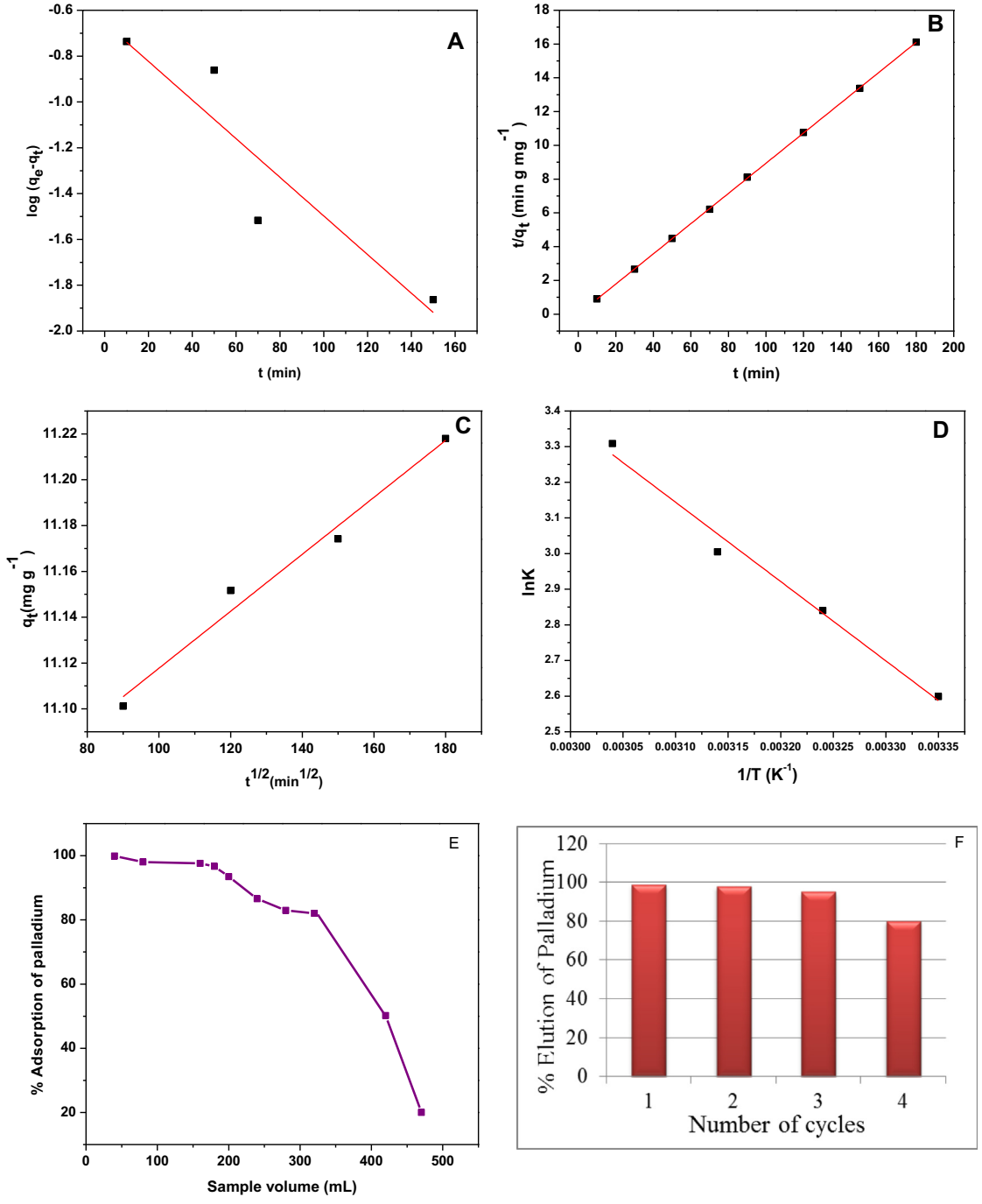

Fig. 6. (A) Pseudo-first-order kinetic plot, (B) pseudo-second-order kinetic plot, (C) plot of q_t versus square root of time, (D) Van't Hoff plot of ln K against $1/T$, (E) effect of sample volume and (F) adsorbent regeneration.

Table 2
Kinetic parameters for the adsorption of palladium(II).

Conc. of Pd(II) solution (mg L^{-1})	q_e (mg g^{-1})	Pseudo first order kinetic model			Pseudo second order kinetic model			Intraparticle diffusion model
		k_1 (min^{-1})	q_1 (mg g^{-1})	R^2	k_2 (g mg min^{-1})	q_2 (mg g^{-1})	R^2	k_{int} (g mg^{-1}) ($min^{0.5}$)$^{-1}$
40	11.304	0.0194	4.5149	0.78	2.004	11.176	0.99	0.0012

$$\ln K = \frac{-\Delta H^0}{RT} + \frac{\Delta S^0}{R} \quad (13)$$

$$\Delta G^0 = -RT \ln K \quad (14)$$

where ΔH^0 and ΔS^0 are enthalpy and entropy changes, R is the universal gas constant (8.314 J mol^{-1} K^{-1}) and T is the absolute temperature (Kelvin). The equilibrium constant K is obtained from the ratio of concentration of Pd(II) adsorbed on the adsorbent material to that in the solution. The slope and intercept of the Van't Hoff plot of ln K against $1/T$ (Fig. 6D) gives the enthalpy and entropy values. The affinity of palladium towards the functionalized resin adsorbent and the feasibility of adsorption process are ascertained through the equilibrium constant K and the Gibb's free energy values. The results are presented in Table 3 and the negative free energy value implies a spontaneous exergonic adsorption process. The magnitude of ΔH^0 serves as a benchmark to know more about the adsorption mechanism and for physical adsorption the value is by and large below 80 kJ mol^{-1} while for strong chemical adsorption the value would fall in the range 80–400 kJ mol^{-1} [40]. The equilibrium constant (K_{ads}) becomes more positive along with the more negative ΔG values at higher temperatures. Consequently, it is evident from these values that higher temperatures augment the adsorption of palladium. The entropy of adsorption was found to be positive and this reflects the increase in randomness at the resin-solution interface. Further, the positive enthalpy change indicates the endothermic interaction between the resin adsorbent and the adsorbate. These values show the efficacy of the AXAD-1180-MBT adsorbent material as a useful adsorbent for palladium(II). The energy of activation (E_a) at different temperatures and the enthalpy of adsorption can be correlated as $E_a = \Delta H_{ads} + RT$ for adsorption from aqueous solutions [41]. The average energy of activation was found to be 21.1067 kJ mol^{-1} and the positive activation energy value also supports the endothermic nature of adsorption process.

3.7. Column study

After optimizing the parameters in batch study, the adsorbent reusability was checked. A glass column 2.5 cm in diameter and 30 cm in length was used for the column adsorption study and 1.0 g of the resin adsorbent material was packed in the glass column. Palladium(II) solution, at a concentration of 40 mg L^{-1} was loaded on to the column while maintaining a flow rate of 6 mL min^{-1}. Pd(II) was effectively adsorbed on the column at pH 4.0, and this was determined using atomic absorption spectrophotometry in the solution phase. From Fig. 6E, it can be seen that beyond 200 mL there is a decline in the percentage of palladium retained in the column. In an adsorption process, regeneration is a crucial aspect and the eluent selected should be able to desorb palladium in a facile manner. Since, palladium is classified as a soft acid, thiourea was selected as an eluent for the desorption [18–20]. Palladium reacts with thiourea to form a stable complex and this reagent effectively disturbs the equilibrium between the resin surface and the adsorbate and this was evident from the yellow color obtained in the eluate. Desorption of palladium from the resin adsorbent column was quantitative with 10 mL of 2% thiourea. The functionalized resin adsorbent could be regenerated and reused for 3 cycles without any drastic reduction in the percentage adsorption (Fig. 6F).

Table 3
Enthalpy, entropy and free energy changes for palladium adsorption.

Temperature (Kelvin)	ΔG^0 (kJ mol^{-1})	ΔS^0 (J mol^{-1} K^{-1})	ΔH^0 (kJ mol^{-1})	E_a (kJ mol^{-1})
298	−6.4161	+83.5039	+18.5045	+21.1067
308	−7.2731			
318	−7.9447			
328	−9.0227			

3.8. Application study in a catalyst

A 5% palladium on activated carbon (spent catalyst) was chosen to study the recovery of palladium. In order to leach palladium, a known weight (0.05 g) of the spent catalyst was taken and digested slowly [42] using a mixture of 10% HCl and 5% H_2O_2 under magnetic stirring. The reaction was carried out for 3 h at 90 °C. The mixture was filtered and the concentration of palladium was checked in the leachate using Atomic absorption spectrophotometry. The pH was adjusted to the optimum value and Pd(II) could be effectively adsorbed onto the adsorbent. The concentration of palladium after adsorption was measured by using AAS. It was observed that Pd(II) could be completely adsorbed onto the surface of the adsorbent. The percentage of palladium adsorbed onto AXAD-1180-MBT was found to be 90.5 ± 0.02% from spent catalyst.

3.9. Adsorption capacity comparison against other matrices

The efficiency of 2-mercaptobenzothiazole impregnated amine functionalized resin was correlated with regard to its adsorption capacity against some of the recently reported solid phase adsorbents [19,20,43–48]. As evident from Table 4, the results demonstrate that 2-mercaptobenzothiazole impregnated amine functionalized resin sorbent has good adsorption capacity as compared to some of the other adsorbents reported in literature. However, in contrast to glycine modified cross linked chitosan and chitosan-tannin extract, the adsorption capacity of AXAD-1180-MBT adsorbent is relatively lower and this could be attributed to the fact that chitosan has NH_2 and OH groups which facilitate good interaction with palladium. Langmuir adsorption capacity is one of the factors that serve as a measure to assess the adsorption efficiency. Nevertheless, several other factors such as reusability, stability and application to real samples are also equally important to judge the performance of the adsorbent. The MBT-resin adsorbent has a reasonably high adsorption capacity of 50 mg g^{-1} and also in the adsorbent preparation, the functionalization of the resin is simple and ensures good reproducibility in the adsorption data. Furthermore, in terms of stability, regeneration and practical

Table 4
Adsorption capacity comparison against other matrices.

SL. No.	Adsorbent material	Adsorption capacity (mg g^{-1})	References
1.	2-Mercaptobenzothiazole impregnated cellulose	5.00	[19]
2.	2-Mercaptobenzimidazole impregnated chitosan	19.26	[20]
3.	Immobilized tannin	27.50	[43]
4.	Activated carbon	35.70	[44]
5.	Biopolymer modified activated carbon	43.50	[44]
6.	Racomitrium lanuginosum biomass	37.20	[45]
7.	Murexide functionalized halloysite nanotubes	42.86	[46]
8.	Glycine modified cross linked chitosan resin	120.39	[47]
9.	Chitosan grafted persimmon tannin	330.00	[48]
10.	2-Mercaptobenzothiazole impregnated amine functionalized resin	50.00	Present study

application to a real catalyst, the functionalized resin has proven to be very effective for the adsorption of palladium.

4. Conclusions

The work described has shown the utility of a sulfur containing ligand anchored onto a macroreticular amine functionalized resin for the sequestration of an industrially useful precious metal. The sorption characteristics of palladium were examined through the study of pH effect, adsorbent dosage, contact time and temperature. The optimum pH for the adsorption of Pd(II) was found to be 4.0. The resin adsorbent exhibits an adsorption capacity of 50.00 mg g^{-1} and the experimental data were explained well with a high regression coefficient through the linear Langmuir adsorption isotherm model and pseudo second order kinetics. The exergonic, increased randomness at the resin-solution interface and endothermic nature of adsorption were ascertained through the sorption thermodynamics. The functionalized resin adsorbent could be effectively regenerated by treating with 2% thiourea and was checked for its applicability to test the adsorption of palladium from a spent catalyst. In addition, this resin-sulfur ligand combination would also be quite useful to recover palladium from electronic components such as printed circuit boards and in nuclear industry for the sequestration of palladium from high level radioactive waste generated from spent nuclear fuel processing.

Acknowledgments

We acknowledge the financial support from University Grants Commission, New Delhi, India (Project No: F.No.41-212/2012 (SR). Thanks to ARCI, Hyderabad, India for their valuable assistance in characterization of the samples for SEM and EDX.

Appendix A. Supplementary data

Supplementary data associated with this article can be found, in the online version, at http://dx.doi.org/10.1016/j.cej.2015.08.061.

References

[1] C.C.J. Seechurn, M.O. Kitching, T.J. Colacot, V. Snieckus, Palladium-catalyzed cross-coupling: a historical contextual perspective to the 2010 Nobel Prize, Angew. Chem. Int. Ed. 51 (2012) 5062–5085.
[2] L. Liu, S. Liu, Q. Zhang, C. Li, C. Bao, X. Liu, P. Xiao, Adsorption of Au(III), Pd(II), and Pt(IV) from aqueous solution onto graphene oxide, J. Chem. Eng. Data 58 (2013) 209–216.
[3] R.M. Izatt, S.R. Izatt, N.E. Izatt, K.E. Krakowiak, R.L. Bruening, L. Navarro, Industrial applications of molecular recognition technology to separations of platinum group metals and selective removal of metal impurities from process streams, Green Chem. 17 (2015) 2236–2245.
[4] D. Parajuli, H. Kawakita, K. Inoue, M. Funaoka, Recovery of gold(III), palladium (II), and platinum(IV) by aminated lignin derivatives, Ind. Eng. Chem. Res. 45 (2006) 6405–6412.
[5] M. Hartings, Reactions coupled to palladium, Nat. Chem. 4 (2012) 764.
[6] V.K. Gupta, C.K. Jain, I. Ali, M. Sharma, V.K. Saini, Removal of cadmium and nickel from wastewater using bagasse fly ash—a sugar industry waste, Water Res. 37 (2003) 4038–4044.
[7] V. Camel, Solid phase extraction of trace elements, Spectrochim. Acta B 58 (2003) 1177–1233.
[8] L. Liu, C. Li, C. Bao, J. Qiong, X. Pengfei, X. Liu, Q. Zhang, Preparation and characterization of chitosan/graphene oxide composites for the adsorption of Au(III) and Pd(II), Talanta 93 (2012) 350–357.
[9] F. Bai, G. Ye, G. Chen, J. Wei, J. Wang, J. Chen, Highly selective recovery of palladium by a new silica-based adsorbent functionalized with macrocyclic ligand, Sep. Purif. Technol. 106 (2013) 38–46.
[10] A. Islam, M.A. Laskar, A. Ahmad, Characterization and application of 1-(2-pyridylazo)-2-naphthol functionalized Amberlite XAD-4 for preconcentration of trace metal ions in real matrices, J. Chem. Eng. Data 55 (2010) 5553–5561.
[11] S.D. Alexandratos, Ion-exchange resins: a retrospective from industrial and engineering chemistry research, Ind. Eng. Chem. Res. 48 (1) (2009) 388–398.
[12] E. Mladenova, I. Karadjova, D.L. Tsalev, Solid-phase extraction in the determination of gold, palladium, and platinum, J. Sep. Sci. 35 (2012) 1249–1265.
[13] Z. Hubicki, A. Wołowicz, Adsorption of palladium (II) from chloride solutions Amberlyst A 29 and Amberlyst A 21 resins, Hydrometallurgy 96 (2009) 159–165.
[14] S. Hoshi, H. Fujisawa, K. Nakamura, S. Nakata, M. Uto, K. Akatsuka, Preparation of Amberlite XAD resins coated with dithiosemicarbazone compounds and preconcentration of some metal ions, Talanta 41 (1994) 503–507.
[15] R. Ruhela, K.K. Singh, B.S. Tomar, J.N. Sharma, M. Kumar, R.C. Hubli, A.K. Suri, Amberlite XAD-16 functionalized with 2-acetyl pyridine group for the solid phase extraction and recovery of palladium from high level waste solution, Sep. Purif. Technol. 99 (2012) 36–43.
[16] K. Fujiwara, A. Ramesh, T. Maki, H. Hasegawa, K. Ueda, Adsorption of platinum (IV), palladium (II) and gold (III) from aqueous solutions onto L-lysine modified cross-linked chitosan resin, J. Hazard. Mater. 146 (2007) 39–50.
[17] C.R. Adhikari, D. Parajuli, K. Inoue, K. Ohto, H. Kawakita, H. Harada, Recovery of precious metals by using chemically modified waste paper, New J. Chem. 32 (2008) 1634–1641.
[18] A.S.K. Kumar, S. Sharma, R.S. Reddy, M. Barathi, N. Rajesh, Comprehending the interaction between chitosan and ionic liquid for the adsorption of palladium, Int. J. Biol. Macromol. 72 (2015) 633–639.
[19] S. Sharma, N. Rajesh, 2-Mercaptobenzothiazole impregnated cellulose prepared by ultrasonication for the effective adsorption of precious metal palladium, Chem. Eng. J. 241 (2014) 112–121.
[20] S. Sharma, M. Barathi, N. Rajesh, Efficacy of a heterocyclic ligand anchored biopolymer adsorbent for the sequestration of palladium, Chem. Eng. J. 259 (2015) 457–466.
[21] V.A. Lemos, P.X. Baliza, Amberlite XAD-2 functionalized with 2-aminothiophenol as a new sorbent for on-line preconcentration of cadmium and copper, Talanta 67 (2005) 564–570.
[22] N. Rajesh, A.S.K. Kumar, S. Kalidhasan, V. Rajesh, Trialkylamine impregnated macroporous polymeric sorbent for the effective removal of chromium from industrial wastewater, J. Chem. Eng. Data 56 (2011) 2295–2304.
[23] M.F. Cheira, Synthesis of pyridylazo resorcinol – functionalized Amberlite XAD-16 and its characteristics for uranium recovery, J. Environ. Chem. Eng. 3 (2015) 642–652.
[24] I.W. Mwangi, J.C. Ngila, J. Kamau, J. Okonkwo, Adsorption Studies of Lead, Copper and Cadmium Ions in Aqueous Solution by Ethylene Diamine Modified Amberlite XAD-1180, Chemistry for Sustainable Development, Springer, 2012. pp. 335–352.
[25] D. Kara, A. Fisher, S.J. Hill, Comparison of some newly synthesized chemically modified Amberlite XAD-4 resins for the preconcentration and determination of trace elements by flow injection inductively coupled plasma-mass spectrometry (ICP-MS), Analyst 131 (2006) 1232–1240.
[26] Z. Hubicki, A. Wołowicz, A comparative study of chelating and cationic ion exchange resins for the removal of palladium (II) complexes from acidic chloride media, J. Hazard. Mater. 164 (2009) 1414–1419.
[27] I. Langmuir, The adsorption of gases on plane surface of glass, mica and platinum, J. Am. Chem. Soc. 40 (1918) 1361–1403.
[28] X. Zou, J. Pan, H. Ou, X. Wang, W. Guan, C. Li, Y. Yan, Y. Duan, Adsorptive removal of Cr(III) and Fe(III) from aqueous solution by chitosan/attapulgite composites: equilibrium, thermodynamics and kinetics, Chem. Eng. J. 167 (2011) 112–121.
[29] K.K. Singh, R. Ruhela, A. Das, M. Kumar, A.K. Singh, R.C. Hubli, P.N. Bajaj, Separation and recovery of palladium from spent automobile catalyst dissolver solution using dithiodiglycolamide encapsulated polymeric beads, J. Environ. Chem. Eng. 3 (2015) 95–103.
[30] H.M.F. Freundlich, Over the adsorption in solution, Z. Phys. Chem. 57 (1906) 385–470.
[31] F. Haghseresht, G. La, Adsorption characteristics of phenolic compound onto coal-reject-derived adsorbents, Energy Fuels 12 (1998) 1100–1107.
[32] J. Febrianto, A.N. Kosasih, J. Sunarso, Y.H. Ju, N. Indraswati, S. Ismadji, Equilibrium and kinetic studies in adsorption of heavy metals using bio sorbent: a summary of recent studies, J. Hazard. Mater. 162 (2009) 616–645.
[33] S. Lagergren, Zur theorie der sogennanten adsorption geloster stoffe, K. Sven. Vetenskapsakad. Handl. 24 (1898) 1–39.
[34] Y.S. Ho, G. Mckay, A multi-stage batch adsorption design with experimental data, Adsorpt. Sci. Technol. 17 (1999) 233–243.
[35] H.K. Boparai, M. Joseph, D.M. Ocarroll, Kinetics and thermodynamics of cadmium ion removal by adsorption onto nanozerovalent iron particles, J. Hazard. Mater. 186 (2011) 458–465.
[36] I.A. Sengil, M. Ozacar, H. Turkmenler, Kinetic and isotherm studies of Cu(II) biosorption onto valonia tannin resin, J. Hazard. Mater. 162 (2009) 1046–1052.
[37] W.J. Weber, J.C. Morris, Kinetics of adsorption on carbon from solution, Sanit. Eng. Div. Am. Soc. Civ. Eng. 89 (1963) 31–60.
[38] K.G. Bhattacharyya, S.S. Gupta, Adsorption of chromium (VI) from water by clays, Ind. Eng. Chem. Res. 45 (2006) 7232–7240.
[39] K.Q. Li, X.H. Wang, Adsorptive removal of Pb(II) by activated carbon prepared from *Spartina alterniflora*: Equilibrium, kinetics and thermodynamics, Bioresour. Technol. 100 (2009) 2810–2815.
[40] X.E. Shen, X.Q. Shan, D.M. Dong, X.Y. Hua, G. Owens, Kinetics and thermodynamics of sorption of nitroaromatic compounds to as-grown and oxidized multiwalled carbon nanotubes, J. Colloid Interface Sci. 330 (2009) 1–8.
[41] A.S.K. Kumar, S. Kalidhasan, V. Rajesh, N. Rajesh, Application of cellulose-clay composite biosorbent toward the effective adsorption and removal of chromium from industrial wastewater, Ind. Eng. Chem. Res. 51 (2012) 58–69.
[42] M.A. Barakat, M.H.H. Mahmoud, Y.S. Mahrous, Recovery and separation of palladium from spent catalyst, Appl. Catal. A 301 (2006) 182–186.

[43] H. Ma, X. Liao, X. Liu, B. Shi, Recovery of platinum (IV) and palladium (II) by bayberry tannin immobilized collagen fiber membrane from water solution, J. Membr. Sci. 278 (2006) 373–380.
[44] H. Sharififard, M. Soleimani, F.Z. Ashtiani, Evaluation of activated carbon and bio-polymer modified activated carbon performance for palladium and platinum removal, J. Taiwan. Inst. Chem. E. 43 (2012) 696–703.
[45] A. Sari, D. Mendil, M. Tuzen, M. Soylak, Biosorption of palladium(II) from aqueous solution by moss (*Racomitrium lanuginosum*) biomass: equilibrium, kinetic and thermodynamic studies, J. Hazard. Mater. 162 (2009) 874–879.
[46] R. Li, Q. He, Z. Hu, S. Zhang, L. Zhang, X. Chang, Highly selective solid-phase extraction of trace Pd(II) by murexide functionalized halloysite nanotubes, Anal. Chim. Acta 713 (2012) 136–144.
[47] A. Ramesh, H. Hasegawa, W. Sugimoto, T. Maki, K. Ueda, Adsorption of gold (III), platinum(IV) and palladium(II) onto glycine modified crosslinked chitosan resin, Bioresour. Technol. 99 (2008) 3801–3809.
[48] Z. Zhou, F. Liu, Y. Huang, Z. Wang, G. Li, Biosorption of palladium(II) from aqueous solution by grafting chitosan on persimmon tannin extract, Int. J. Biol. Macromol. 77 (2015) 336–343.